Modeling of 16×10 Gbps integrated OAM-MDM based IsOWC system using improved ZCC-OCDMA code

MEET KUMARI*
Department of ECE, UIE, and UCRD, Chandigarh University, Mohali-140413, Punjab, India

In this paper, an integrated 16×10 Gbps mode-division-multiplexing and optical-code-division-multiple access (MDM-OCDMA) technique based inter-satellite optical wireless communication (IsOWC) model is presented. To enhance the system security and capacity, different orbital angular momentum (OAM) beams and distinct improved zero cross-correlation code sequences are transmitted. The results exhibit that the proposed model offers 36,000 km range with 8.10e-8 watt signal power. The system can sustains spot size of 15 μm and offers massive capacity at 25 cm aperture diameter. Moreover, the system offers better performance than existing codes supporting 128 end-users at 0.5-5 dB additional loss with 15 μrad divergence angle providing 95.94 dB gain and 21.45 dB signal-to-noise-ratio.

(Received January 20, 2025; accepted August 4, 2025)

Keywords: IsOWC, MDM, OAM, OCDMA, Improved ZCC

1. Introduction

With the continuous usage of high-speed Internet, live streaming, video-conferencing, etc., the bandwidth & capacity demands have been raised dramatically [1]. Also, considering the tremendous growth of remarkably dynamic traffic patterns owing to rise of real-time gaming, social networking, and high definition video streaming in modern networks, flexible resource allocation is significant for cost saving as well as revenue generation [2].

Further, advancement in satellite communication and realization of more developed satellite-based instruments illustrate modern designs of inter-satellite optical wireless communication (IsOWC). Owing to rising demands for high traffic rate and huge communication capacity, there is a need to actively work on IsOWC based architectures [1]. For IsOWC systems, spatial division multiplexing (SDM) is potentially utilized to improve the number of inter-satellite links for independent transmission of data. Orbital angular momentum (OAM) is considered as another SDM technique is to utilize the light field spatial distribution. It is an orthogonal light spatial modal which enables IsOWC system with massive capacity [3–5].

Moreover, optical code division multiple access (OCDMA) is an innovative technology for IsOWC considering its characteristics like asynchronous operation, protocol transparency, high network flexibility, simplified network realization as well as potentially improved security. But the interference among OCDMA codes i.e. multiple access interference (MAI), could be a constraint in the simultaneous users data transmission by different code users [6–8].

1.1. Related work

Recently, Tawfik et al. designed an IsOWC system comprising the on-off keying (OOK) modulation over a 45,000 km range at 2 Gbps transmission rate [9]. Even with larger transceiver aperture diameter of 30 cm, it offers low data rate of 16×2 Gbps. Sharma and Kumar proposed an IsOWC system providing high bandwidth, low power, small size, low cost and light weight architecture. The results exhibit faithful transmission range of 1000 km at limited throughput of 2.5 Gbps [10]. Due to larger divergence angle of 2 mard, it offers lower aggregate data rate of 2.5 Gbps for lower orbit satellites. Youssouf et al. realized an IsOWC system incorporating binary phase shift keying (BPSK) scheme. The results depict the successful inter-satellite distance of 1000 km at 10 Gbps throughput employing an optical amplifier [11]. But, this system is realized without considering thermal noise, additional loss and beam divergence. Patnaik and Sahu present an IsOWC system incorporating quadrature phase-shift keying (QPSK) modulation. The results illustrate the faithful inter-satellite distance of 9532 km at 100 Gbps throughput [12]. But due to the presence of complex receiver detection by using QPSK scheme, it enhances the system complexity and cost. Gill et al. proposed a 64 Laguerre-Gaussian (LG) modal mode division multiplexing (MDM) IsOWC system incorporating modified duobinary return to zero (MDRZ) basics differential QPSK (DQPSK) modulation scheme. The results exhibit maximum inter-satellite distance of 4500 km distance at 10 Gbps bit rate [13]. However, it offer higher data rate of 64×10 Gbps, but considering complex and costlier detection schemes. Sachdeva et al. [7] presents a hybrid MDM-OCDMA scheme in IsOWC system. The results depict that the system offers 5000 km transmission distance at 120 Gbps data rate using optical

amplifiers for both LG and Hermite-Gaussian (HG) modes. This system can be used for lower earth orbits owing to limited transmission range. Hamadamen et al. analyzed a 16-channel IsOWC system comprising optical amplifier. The results exhibits maximum inter-satellite range of 3600 km at 64 Gbps throughput [14]. With simple and cost-effective system design it provides limited transmission range even at lower divergence angle of 0.75 μrad. Gill et al. proposed a MDM-IsOWC system utilizing Manchester, differential phase shift keying (DPSK), and DQPSK modulation methods. The results exhibits faithful inter-satellite range of 3750 km at high date rate of 40 Gbps using DQPSK modulation [15]. In spite of providing higher data rate of 64×40 Gbps data rate, it also increases receiver complexity and system cost. From previous works, it is depicted that existing IsOWC systems undergo several challenges like limited data rate, large distance, limited system capacity and hardware complexity.

1.2. Motivation

The IsOWC systems offer many advantages for future based communication systems such as higher throughput, less payload, low power requirement, smaller terminal size as well as and weight. As compared to conventional microwave inter-satellite communication scenario, IsOWC enables optical link communication as a promising technology to fulfill the increasing demands of high-speed transmission having massive data in space [16]. IsOWC using OCDMA scheme is believed as good candidate to offer link security [17]. Again, massive IsOWC transmission is critical owing to the design complexity and high cost of the space communication. Also, the presence of various link losses and impairments such as beam divergence, pointing errors, additional losses and receiver noise, are not explored in details in previous works. Meanwhile, a new OCDMA code is also proposed namely improved zero cross correlation (ZCC) code to secure the data and to support larger number of users having zero cross-correlation and maximum auto-correlation characteristics. In short, a hybrid MDM/OCDMA based IsOWC system using different OAM beams is served as high diversity IsOWC model.

1.3. Contributions

Major contributions of the proposed model are given as:

- Design an improved ZCC OCDMA code and realized it in an intergrated MDM/OCDMA scheme based IsOWC system using OAM beams.
- To realized the system employing different OAM beams {[0,0], [0,1], [0,2], [0,3]} for long-reach high-speed inter-satellite link.
- To investigate the system performance for varied spot size, transmission distance, additional link losses, transceiver aperture diameters and beam divergence in terms of eye opening, signal power, error rate, quality factor, timing as well as optical spectra.
- To compare the proposed code with other codes considering additional and beam divergence for 128 simultaneous end users.
- To validate the system perfirmance with existing works based on different parameters.

Fig. 1 depicts the conceptual diagram of IsOWC system for low Earth orbit (LEO), medium Earth orbit (MEO) and geostationary Earth orbit (GEO) orbital satellites.

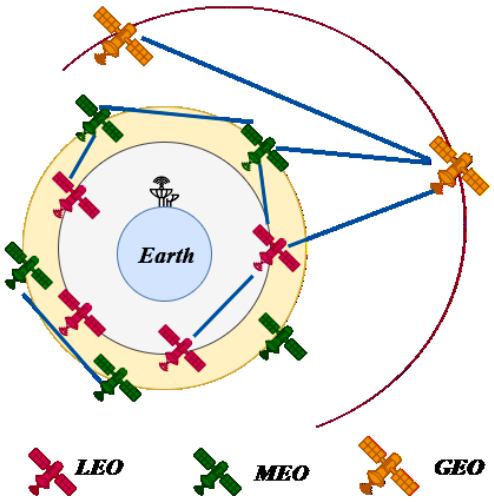

Fig. 1. Conceptual diagram of IsOWC (colour online)

1.4. Paper organization

This work is structured as: Section 2 illustrates the proposed IsOWC system using integrated MDM/OCDMA system along with simulation parameters and generated modes. Section 3 exhibits the numerical analysis of the improved ZCC code along with impact of various system parameters in the proposed model. Lastly, the conclusion with future work is presented in Section 4.

2. Proposed IsOWC using OAM-MDM/OCDMA system

Fig. 2(a) and 2(b) illustrate the proposed IsOWC system using OAM-MDM/OCDMA scheme and generated OAM mode profiles. Here, existing ZCC code is modified as improved ZCC code and realized in the system. Four different OAM modes viz. OAM[0,0], OAM[0,1], OAM[0,2] and OAM[0,3] are transmitted for LEO-MEO-GEO inter-satellite links using OptiSystem v.20 tool. Four transceivers providing total sixteen integrated modal and coded signals are realized using OOK modulation for 1550-1555.6 nm wavelength band with 0.8 nm channel spacing. Four encoders are incorporated per transceiver, where each encoder multiplex the two specific incoming light signals from two laser diodes (LDs) as per code sequence. Then this wavelength division multiplexing (WDM) multiplexed

signal is forward to a Mach-Zehnder modulator at 10 Gbps-non return to data format. The generated OAM modes are described as [18]:

$$\omega_{s,d}(r,\emptyset) = \alpha\left(\frac{2r^2}{\rho_0^2}\right)^{\frac{\theta}{2}}.G_s^d\left(\frac{2r^2}{\rho_0^2}\right).exp\left(\frac{-r^2}{\rho_0^2}\right).exp\left(\frac{\pi r^2}{\lambda R_0}\right) \quad (1)$$

$$\begin{cases}\cos(d\emptyset), d < 0\\ \sin(d\emptyset), d \geq 0\end{cases}$$

where r means curvature radius, s and d indicate x-and y-axis modes dependencies considerably, ρ_0 indicates spot size, G_s and G_d mean Laguerre polynomials, R_0 is the normalized radius, θ is beam divergence angle and α is atmospheric attenuation [18].

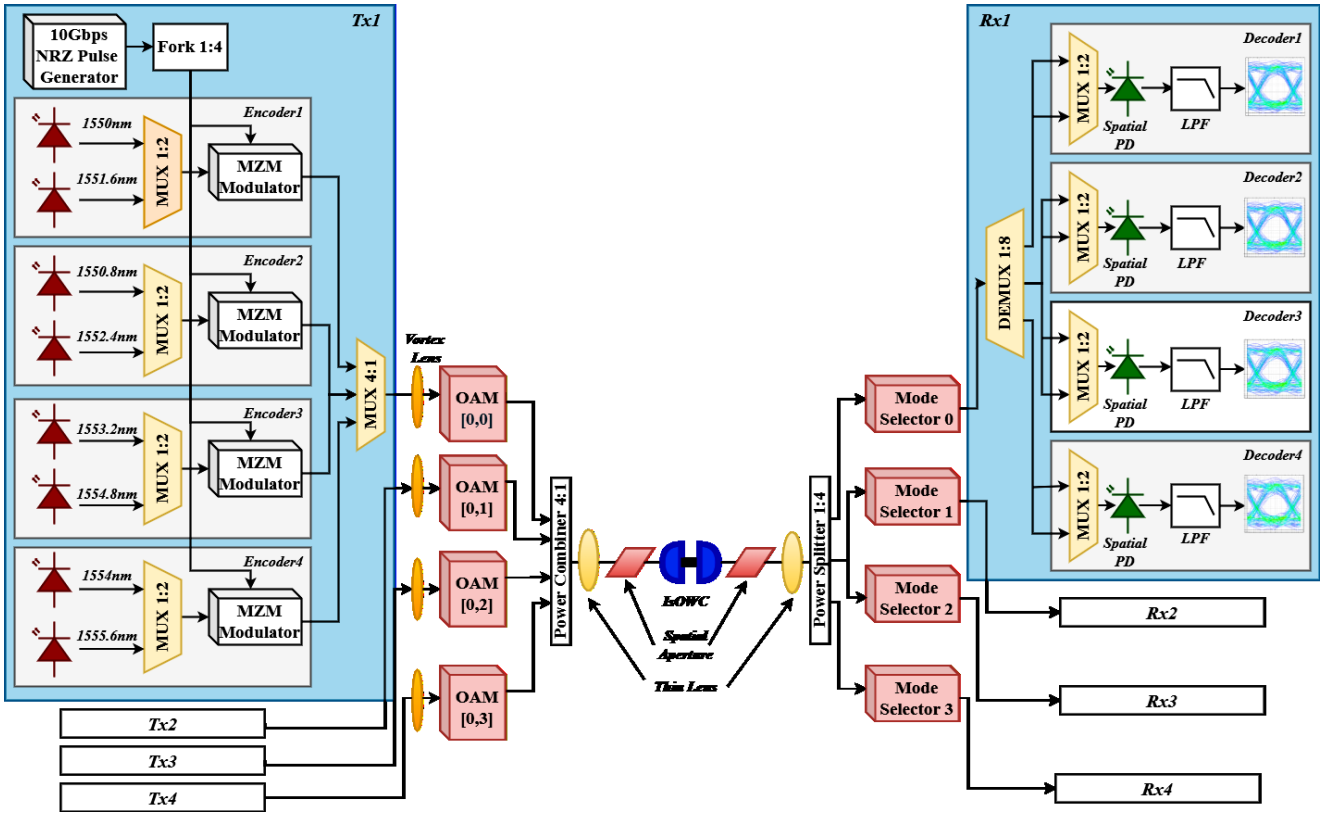

(a)

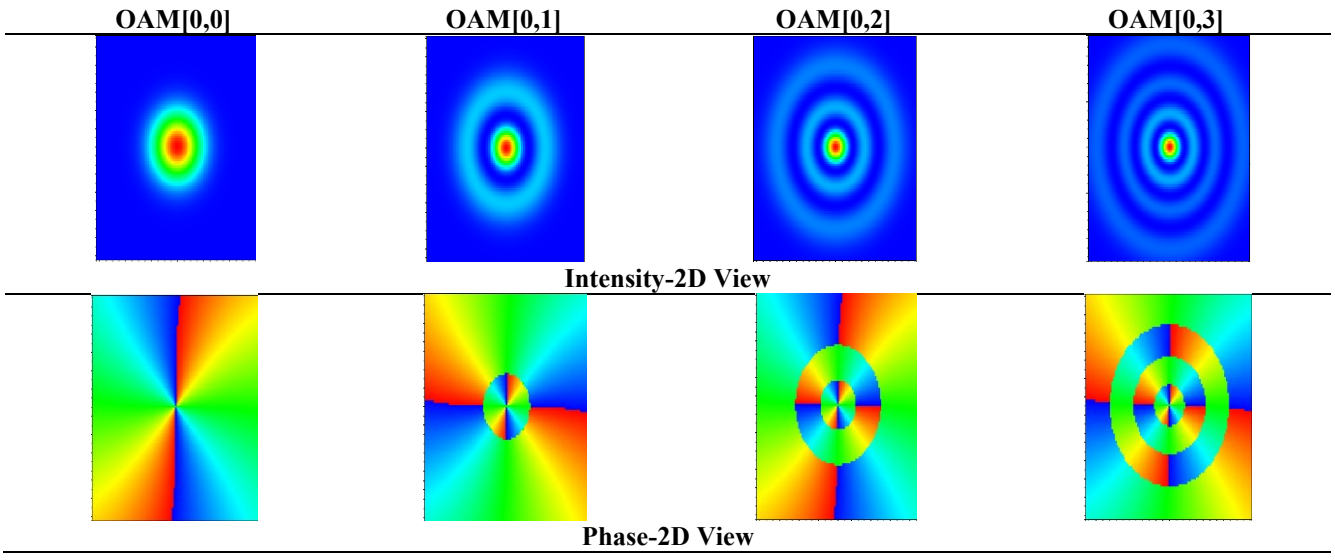

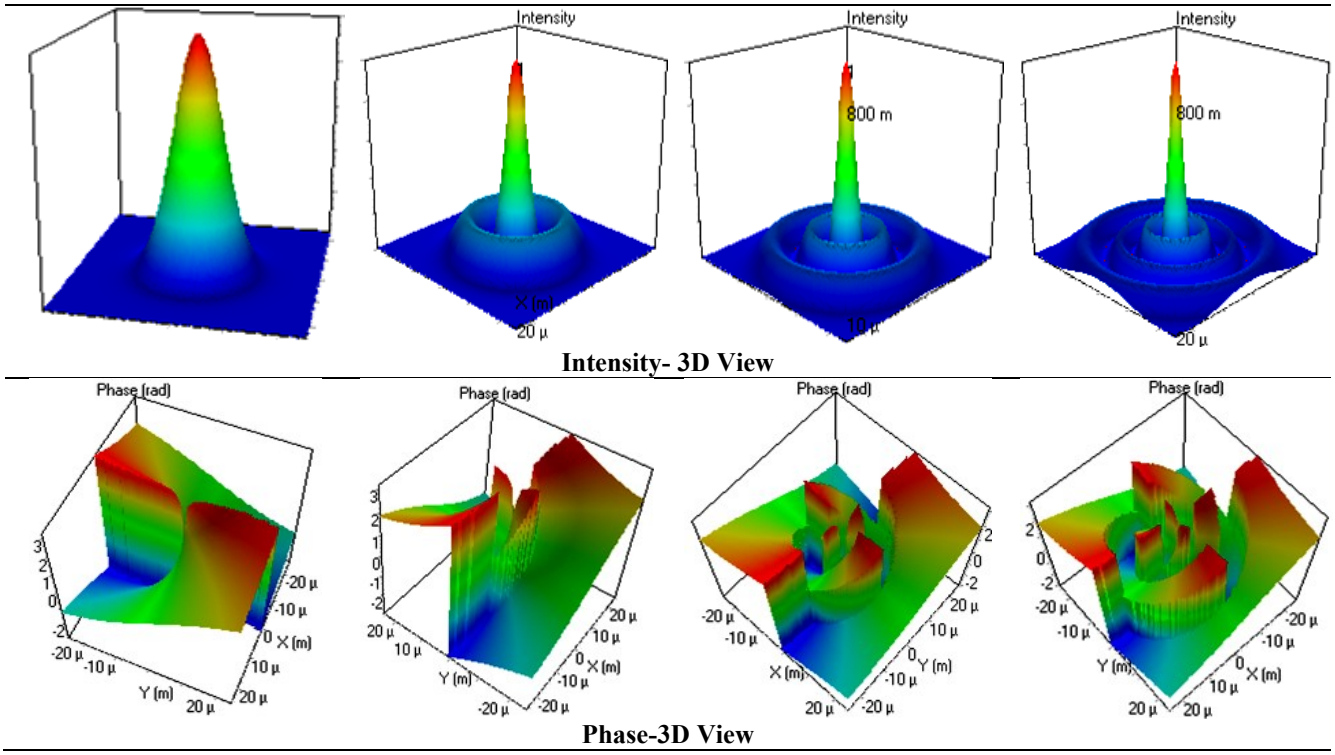

(b)

Fig. 2. (a) Setup of IsOWC system using integrated MDM/OCDMA technique and (b) generated OAM modes' profiles (colour online)

Likewise, other encoded data is collected by a 4:1 WDM multiplexer followed by a vortex lens for a phase transformation to OAM mode profiles, and affecting the beam focus. After this, sixteen different OAM beams operated by improved ZCC unique code sequence are realized by using different mode generator and then passed to the IsOWC link by using a 1:4 power combiner. A set of a thin lens (focal length=10 mm) and a spatial aperture (width=10 µm) are utilized over an IsOWC link to apply a phase transformation and a circular or square window to the transverse modes respectively.

Further, sixteen receiver sections are utilized for different decoders corresponding to distinct modes profiles. Here, for signals are splitted into mode selectors via a 1:4 power splitter followed by a 1:8 WDM demultiplexer per operating mode and then signals are transferred to distinct decoder. Each decoder comprises of a 2:1 WDM multiplexer as per code sequence, a spatial photodiode and a low pass filter. Finally, to evaluate the system performance, a bit error rate (BER) analyzer is used at each user end. The main parameters of the proposed IsOWC model are tabulated in Table 1.

Table 1. Simulation parameters of the proposed IsOWC model [19]

Parameters	**Value**	**Unit**
Input power	20	dBm
Wavelength	1550-1555.6	nm
Throughput	10	Gbps
Geometric loss	Yes	
Tx/Rx aperture diameter	25-70	cm
Channel spacing	0.8	nm
Responsivity (R)	1	A/W
Dark current	9	nA
Filter order	4	
Filter cut off frequency	7.5	GHz
Electric charge (e)	1.602×10^{-19}	C
Distance	27000-36000	km
Thermal noise	1×10^{-27}	W/Hz
Temperature (T_n)	300	K
Electrical bandwidth (B)	311×10^{6}	Hz
Resistance (R_L)	1030	Ω
Boltzmann constant (K_b)	1.38×10^{-23}	J/K
Tx/Rx beam divergence	0.0015-0.0024	mrad
Spot size	10-15	µm
Beam divergence	0.002-15	µrad
Additional loss	0.5-5	dB
No. of users	128	
Code weight	2	
Code length	8	

3. Results and discussion

In this proposed work, the improved ZCC code is designed. The improved ZCC code is presented in a matrix of $K \times N$, where $K \rightarrow$ number of users (rows) and $N \rightarrow$ code length (columns). The basic ZCC code design based on this matrix with weight, W=1 is represented as $(K = 2, W = 1, N = 1)$ [20]:

$$ZCC_{W=1} = \begin{Bmatrix} 1 & 0 \\ 0 & 1 \end{Bmatrix} \quad (2)$$

Also, to transform this code from W=1 to $W = n$, the general form is given as:

$$ZCC_{W=n} = \left(\begin{array}{c|c} A & B \\ C & D \end{array}\right) \quad (3)$$

where $n \rightarrow$ code-weight integer value.
where $[A] \rightarrow$ consist of W replication of basic matrix $\sum_{j=1}^{W}(ZCC_{W=1})$, $[B] \rightarrow$ consist of $(n,\ n \times 2)$ matrix of zero. $[C] \rightarrow$ consist of duplication of matrix $[A]$. $[D] \rightarrow$ consist of duplication of matrix $[B]$. For instant, the transformation improved ZCC code from W=1 to $W = 2$, is represented as:

$$ZCC_{W=2} = \begin{Bmatrix} A \rightarrow \begin{Bmatrix} 1 & 0 & 1 & 0 \\ 0 & 1 & 0 & 1 \end{Bmatrix} & B \rightarrow \begin{Bmatrix} 0 & 0 & 0 & 0 \\ 0 & 0 & 0 & 0 \end{Bmatrix} \\ C \rightarrow \begin{Bmatrix} 0 & 0 & 0 & 0 \\ 0 & 0 & 0 & 0 \end{Bmatrix} & D \rightarrow \begin{Bmatrix} 1 & 0 & 1 & 0 \\ 0 & 1 & 0 & 1 \end{Bmatrix} \end{Bmatrix} \quad (4)$$

The relation between K, W and N is given as for $n > 1$

$$Number\ of\ users = W \times 2$$
$$Code\ length = K \times W$$

The proposed ZCC correlation properties is given as [21]:

$$\sum_{j=1}^{n} F_k(i)F_l(i) = \begin{Bmatrix} W, & For\ k = l \\ 0, & Else \end{Bmatrix} \quad (5)$$

where F_k and F_l are two distinct code sequences.

The assumptions utilized to realize the improved ZCC code are as follows [21]:

1. Laser input source is unpolarised incorporating flat spectrum over $\left[f_0 - \frac{\triangle f}{2}, f_0 + \frac{\triangle f}{2}\right]$ spectrum, where f_0 and $\triangle f$ are reference and central frequency respectively.
2. A single spectral component incorporates an equivalent spectral width and equal power is obtained at the receiver.
3. For each user, a single bit stream is synchronized.

Meanwhile, Table 2 illustrates code design for four users having code weight of 2 the code length of eight for operating wavelength from 1550-1555.6 nm with channel spacing of 0.8 nm.

Table 2. Improved ZCC code $(K = 4, W = 2, N = 8)$

User	1550nm	1550.8 nm	1551.6 nm	1552.4 nm	1553.2 nm	1554nm	1554.8 nm	1555.6 nm
1st	1	0	1	0	0	0	0	0
2nd	0	1	0	1	0	0	0	0
3rd	0	0	0	0	1	0	1	0
4th	0	0	0	0	0	1	0	1

The chip position for four users ZCC code is defined as:

$$chip\ positions = \begin{cases} User\ 1 \rightarrow 1,3 \\ User\ 2 \rightarrow 2,4 \\ User\ 3 \rightarrow 5,7 \\ User\ 4 \rightarrow 6,8 \end{cases}$$

It is seen that compared to exiting ZCC codes in refs. [22] and [20], the proposed code is simple to design with less code length for same number of users. Thus, it enhances the system flexibility, reduces system complexity and cost.

Further, the system signal to noise ratio, SNR is evaluated as [20]:

$$SNR = \frac{2\left[\frac{RWP_{sr}}{N}\right]^2}{\left[\frac{P_{sr}eBR}{N}\right](K-1+W)W+\frac{4BK_bT_n}{R_L}} \quad (6)$$

where R, e, B, K_b, T_n and R_L are described in Table 2. Also, P_{sr} is the received power. Meanwhile, the BER is defined as [20]:

$$BER = \frac{1}{2}erfc\sqrt{SNR/8} \quad (7)$$

Again, the received power, P_r in IsOWC is defined as [9]:

$$P_r = P_t\theta_r\theta_t(\lambda/4\pi L)^2G_tG_rR_tR_r \quad (8)$$

where P_t is optical transmitted power, θ_r and θ_t mean optical efficiency at transmitter & receiver respectively, λ is wavelength, L is the transmission range, G_t and G_r indicate the aperture at transmitter and receiver respectively, R_t and R_r mean pointing loss factor at transmitter & receiver respectively. $(\lambda/4\pi L)^2$ defines the free space path loss.

3.1. Impact of varied spot size on the proposed model in terms of Q-factor, eye opening, received signal power and eye patterns

Fig. 3(a) and 3(b) depict the proposed IsOWC system for varied spot size versus Q-factor and eye opening versus signal power respectively, over 30,000 km distance at 160 Gbps data rate. With the increase in OAM mode

and with the increment in spot size, the system performance decreases as Q-factor decreases. At Q-factor limit of value 6, the fundamental mode i.e. OAM[0,0] performs best over others higher order modes.

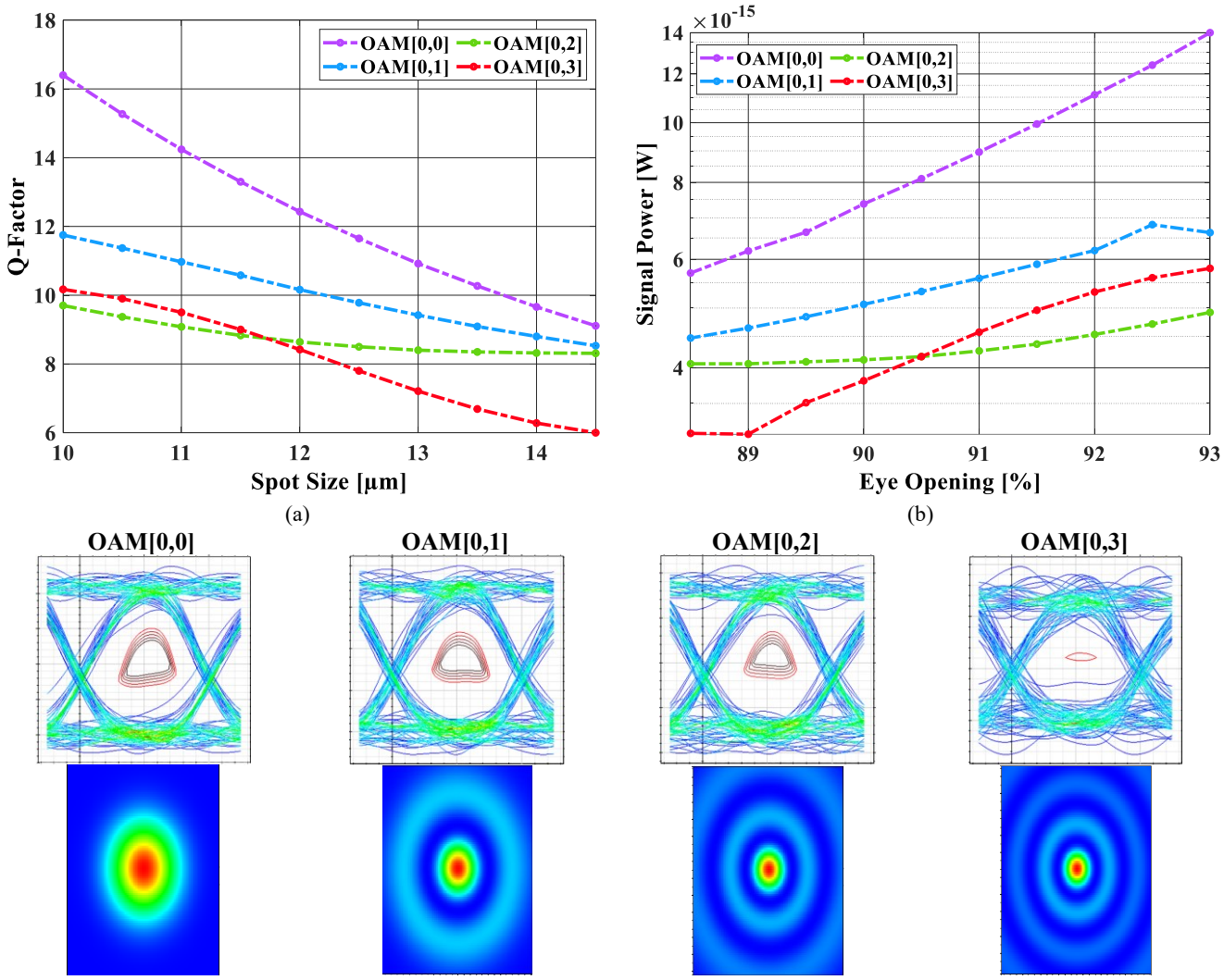

Fig. 3. Performance analysis for varied (a) spot size vs. Q-factor and (b) eye opening vs. received signal power; insets: distinct OAM modes' eye patterns and intensity profiles at spot size of 14.5µm (colour online)

It is noticed that the proposed IsOWC system operating at OAM[0,0], OAM[0,1], OAM[0,2] and OAM[0,3] mode can sustain high spot size exceeding 15, 15 and 15 µm respectively, for all sixteen active users, as shown in Fig. 3(a). However, the worst performance is achieved for OAM[0,3] which indicate limited spot size of 15 µm at acceptable Q-factor of 6. Moreover, Fig. 3(b) depicts that with the rise in eye opening, the signal power also increases. With the eye opening of 88.5% the maximum signal power of 5.57e-8, 4.47e-8, 4.06e-8 and 3.13e-8 W achieved for OAM[0,0], OAM[0,1], OAM[0,2] and OAM[0,3] mode, respectively. Insets indicate the widely opened eye pattern for OAM[0,0], where for other modes, closure eye patterns are obtained at 14.5 µm spot size. Meanwhile, the archived intensity profiles for different OAM modes strengths the above statements. Table 3 depicts the summarized results for varied spot size in the system.

Table 3. Summarized obtained results for varied spot size, eye opening and signal power @Q-factor of 6

Parameter	OAM[0,0]	OAM[0,1]	OAM[0,2]	OAM[0,3]
Maximum spot size (µm)	>15	>15	>15	15
Maximum eye opening (%)	88.5	88.5	88.5	88.5
Signal Power (W)	5.57e-8	4.47e-8	4.06e-8	3.13e-8

3.2. Impact of varied inter-satellite transmission range in terms of Q-factor, eye opening, received signal power, optical spectra and eye patterns

Fig. 4(a) and 4(b) exhibit the proposed IsOWC system for varied transmission range versus Q-factor and eye

opening versus signal power respectively, at 160 Gbps data rate. It is noticed that with the increase in OAM mode value as well as enlarging the transmission range, the IsOWC system performance decays. At Q-factor limit of 6, OAM[0,0] performs best over OAM[0,1] followed by OAM[0,2] and OAM[0,3] modes. Fig. 4(a) exhibits that faithful IsOWC range of more than 36000, 36000, 34000 and 30,000 km for OAM[0,0], OAM[0,1], OAM[0,2] and OAM[0,3] modes is achieved respectively, at Q-factor of 6. Also, Fig. 4(b) exhibits that high signal power is obtained for large eye opening. As depicted, maximum 8.10e-8, 4.28e-8, 2.77e-8 and 2.25e-8 watt for OAM[0,0], OAM[0,1], OAM[0,2] and OAM[0,3] modes is obtained at 92.2% eye opening. Over long distance misalignment causes distinct OAM modes to generate modal crosstalk.

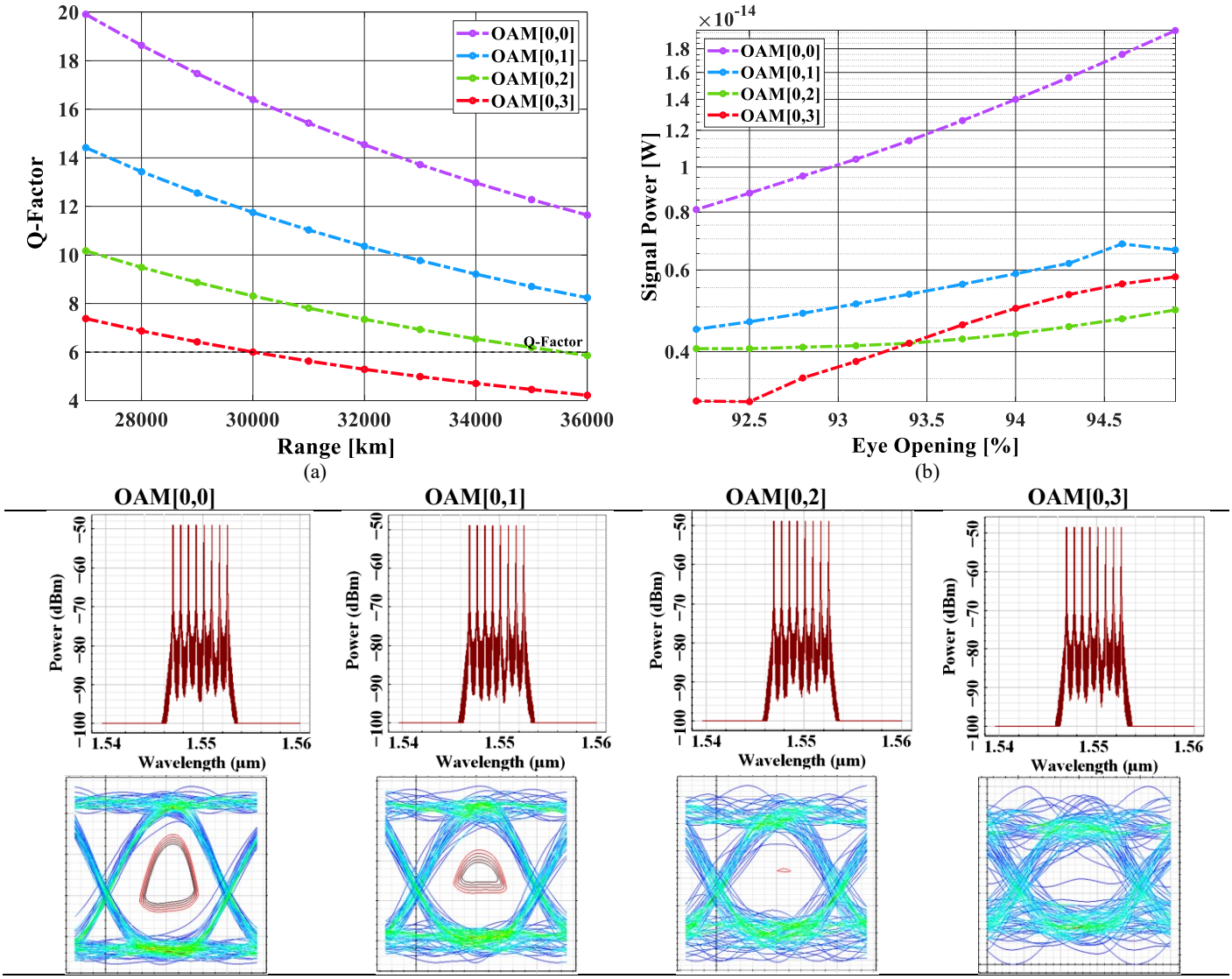

Fig. 4. Performance evaluation for varied (a) inter-satellite range vs. Q-factor and (b) eye opening vs. received signal power; insets: distinct OAM modes' optical spectra and eye patterns at transmission range of 36000 km (colour online)

Also, random fluctuations due to temperature variations distort and spread OAM signals. Thus, a larger aperture is requisite to capture the incoming beams. Also, insets depict the obtained optical spectra for all operating modes and exhibits that out of all modes fundamental mode offers minimum channel interference and noise. Besides, best eye opening is observed for OAM[0,0] followed by higher modes and it strengths the above discussion. Table 4 depicts the summarized results for varied transmission range in the system.

Table 4. Summarized obtained results for varied transmission distance, eye opening and signal power @Q-factor of 6

Parameter	OAM[0,0]	OAM[0,1]	OAM[0,2]	OAM[0,3]
Maximum range (km)	>36,000	~36,000	34,000	30,000
Maximum eye opening (%)	92.2	92.2	92.2	92.2
Signal Power (W)	8.10e-8	4.28e-8	2.77e-8	2.25e-8

3.3. Impact of varied Tx/Rx aperture diameters in terms of Q-factor and eye patterns

Fig. 5(a) and 5(b) exhibit the proposed IsOWC system for varied Tx and Rx aperture diameters over a 30,000 km range at 160 Gbps data rate. It is evident that with the increase in aperture diameters at both Tx and Rx, the Quality factor firstly increases and then decreases for all OAM modes due to link non-linearities. Fig. 5(a) depicts that maximum Q-factor value of 28, 21, 14 and 11 is obtained for OAM[0,0], OAM[0,1], OAM[0,2] and OAM[0,3] modes respectively, at 50 cm Tx aperture diameter. Moreover, Fig. 5(b) exhibits maximum Rx aperture diameter of 50 cm which offers high Q factor value of 27.42, 20.24, 13.95 and 10 for OAM[0,0], OAM[0,1], OAM[0,2] and OAM[0,3] respectively. It is also analyzed that primary OAM mode offers best performance over higher order modes for both varied Tx and Rx aperture diameters.

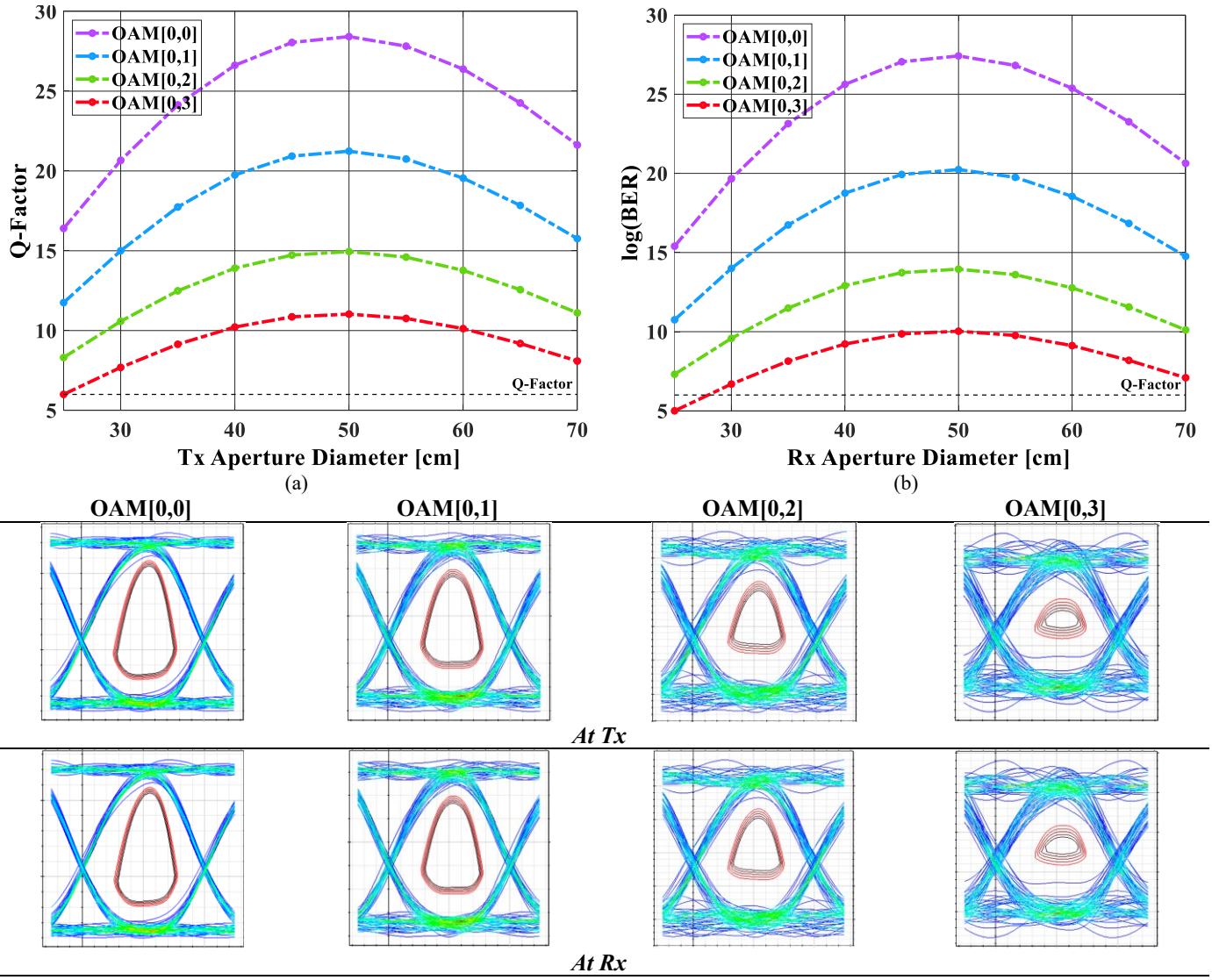

Fig. 5. Performance evaluation for varied aperture diameters at (a) Tx vs. Q-factor and (b) Rx. vs. Q-factor; insets: eye patterns for distinct OAM modes for Tx and Rx aperture diameter of 50 cm (colour online)

Meanwhile, the obtained eye patterns for both Tx and Rx aperture diameters exhibit the optimum performance of system for variable Tx aperture diameter than Rx aperture diameter for all modes. Table 5 depicts the summarized results for varied Tx/Rx aperture diameter in the system.

Table 5. Summarized obtained results for varied aperture diameter at both Tx and Rx

Maximum Q-factor	OAM			
	[0,0]	[0,1]	[0,2]	[0,3]
Tx	28	21	14	11
Rx	27.42	20.24	13.95	10

3.4. Impact of varied Tx/Rx beam divergence in terms of BER and timing diagrams

Fig. 6(a) and 6(b) illustrate the proposed IsOWC system performance for varied beam divergence at both Tx and Rx over a 30,000 km range at 160 Gbps. It is realized that the increment in beam divergence also increases the BER values and thus performance of the proposed IsOWC system diminishes. Acceptable Tx beam divergence of 0.0022, 0.0019, 0.0015 and <0.0015 mrad for OAM[0,0], OAM[0,1], OAM[0,2] and OAM[0,3] modes is achieved respectively, at BER of 10e-9, as depicted in Fig. 6(a). Additionally, Fig. 6(b) illustrates maximum sustainable Rx beam divergence of 0.0021, 0.0018, 0.0014 and <0.0015 mrad for OAM[0,0], OAM[0,1], OAM[0,2] and OAM[0,3] modes is achieved respectively. It is noticed that Rx beam divergence are more susceptible to link noise and MAI interference. Besides, the obtained timing diagrams at Tx and Rx beam divergence of 0.0024 mrad for all operating modes supports the above discussions.

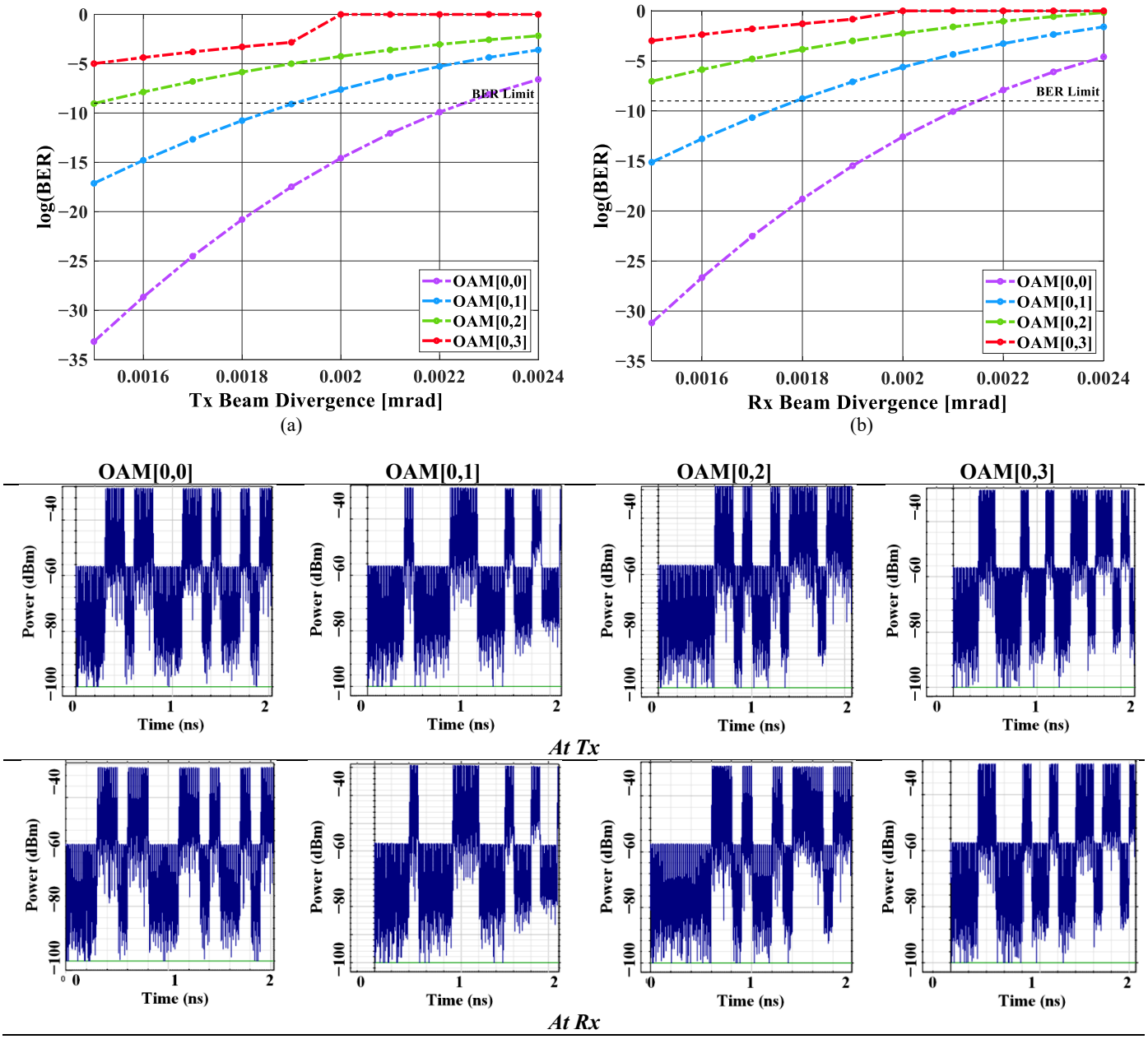

Fig. 6. Performance evaluation for varied beam divergence at (a) Tx vs. BER and (b) Rx. vs. BER; insets: timing diagrams for distinct OAM modes for Tx and Rx beam divergence of 0.0024 mrad (colour online)

Table 6 depicts the summarized results for varied Tx/Rx pointing error in the system. Table 7 depicts obtained results in distinct parameters viz. gain, noise figure, output signal and optical signal to noise ratio (OSNR).

Table 6. Summarized obtained results for varied beam divergence (in mrad) at both Tx and Rx @BER of 10e-9

Maximum divergence (mrad)	OAM			
	[0,0]	[0,1]	[0,2]	[0,3]
Tx	0.0022	0.0019	0.0015	<0.0015
Rx	0.0021	0.0018	0.0014	<0.0015

Table 7. Obtained results

Range (km)	Gain (dB)	Noise Figure (dB)	Output signal (dBm)	OSNR (dB)
26000	95.94	-95.94	-78.54	21.45
28000	95.28	-95.28	-78.88	21.11
30000	93.72	-93.72	-77.36	20.74
32000	93.18	-93.18	-79.64	20.35
34000	87.78	-87.78	-80.05	19.94
36000	85.39	-85.39	-82.45	17.54

3.5. Comparison analysis with other codes

Fig. 7(a) and 7(b) illustrate the proposed system performance for varied additional link loss with transceiver divergence angle of 0.1 and 15 µrad over a 30,000 km range at 160 Gbps data rate. Two OCDMA codes viz. Walsh-Hadamard and double-weight (DW) codes are compared with the proposed code with code weight of 2 supporting 128 simultaneous end users. Tables 8 and 9 depict the design of Walsh-Hadamard and double-weight (DW) codes for fixed code weight of 2. Table 10 illustrates the codes' properties of three different OCDMA codes. Noted that with the increase in additional loss in the IsOWC link having transmitter (=0.1 µrad) and receiver (=15 µrad) divergence angle, the received optical power decreases.

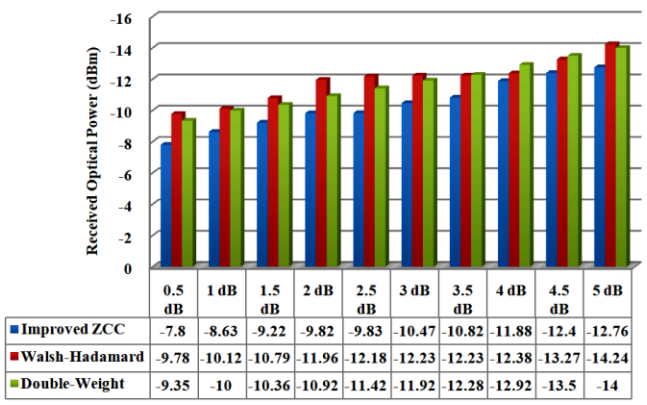

	0.5 dB	1 dB	1.5 dB	2 dB	2.5 dB	3 dB	3.5 dB	4 dB	4.5 dB	5 dB
Improved ZCC	-7.8	-8.63	-9.22	-9.82	-9.83	-10.47	-10.82	-11.88	-12.4	-12.76
Walsh-Hadamard	-9.78	-10.12	-10.79	-11.96	-12.18	-12.23	-12.23	-12.38	-13.27	-14.24
Double-Weight	-9.35	-10	-10.36	-10.92	-11.42	-11.92	-12.28	-12.92	-13.5	-14

(a)

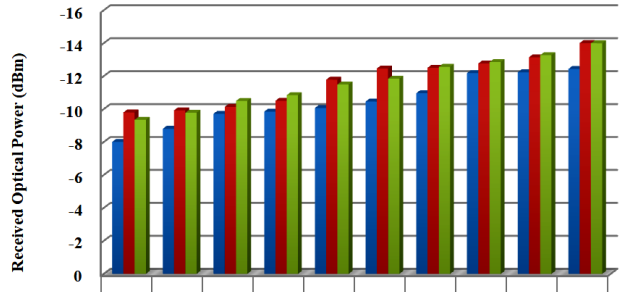

	1	2	3	4	5	6	7	8	9	10
Improved ZCC	-8.01	-8.81	-9.72	-9.85	-10.0	-10.4	-10.9	-12.1	-12.2	-12.4
Walsh-Hadamard	-9.8	-9.93	-10.1	-10.5	-11.7	-12.4	-12.5	-12.7	-13.1	-14.0
Double-Weight	-9.35	-9.78	-10.5	-10.8	-11.5	-11.8	-12.5	-12.8	-13.2	-14

(b)

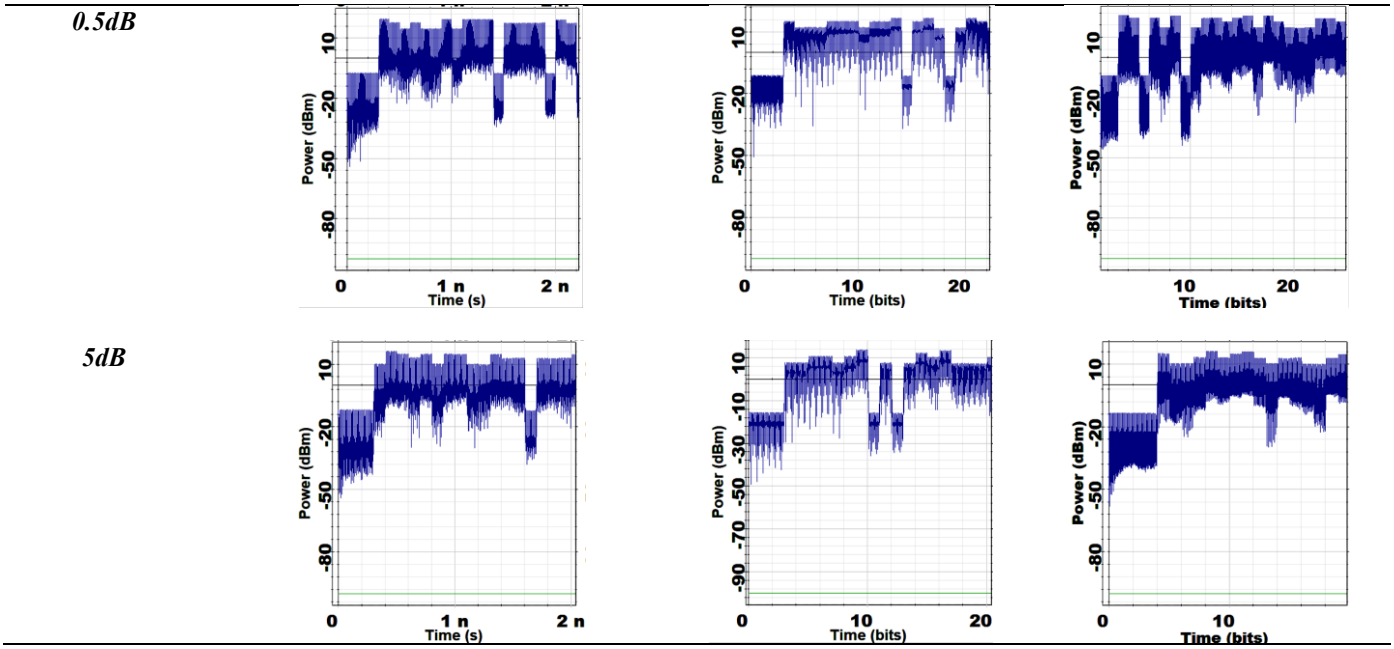

Fig. 7. Comparison performance for the proposed ZCC code with other codes at divergence angle of (a) Tx=0.1 µrad, Rx=15 µrad and (b) Tx=15 µrad, Rx=0.1 µrad for varied additional loss; insets: obtained timing diagrams for different codes (colour online)

As seen, out of all codes, the proposed improved ZCC code offers maximum received power than DW followed by Hadamard code. This is due to favorable zero-cross correlation and maximum correlation properties of improved ZCC code supporting 128 end users as compared other codes. With 0.5-5 dB additional loss, the received power ranges from -7.8 to -12.76 dBm, -9.78 to -14.24 dBm and -9.35 to -14 dBm for improved ZCC, Hadamard and DW codes is obtained, respectively, as seen in Fig. 7(a). Moreover, for transmitter and receiver divergence angle of 15 and 0.1 μrad, maximum received power of -8.01 to -12.44 dBm, -9.8 to -14.01 dBm and -9.35 to -14 dBm for improved ZCC, Hadamard and DW codes is attained, respectively, as seen in Fig. 7(b). The less distorted and clean timing diagrams at 0.5 dB additional loss also supports the above discussions.

Besides this, Table 11 presents the comparison analysis of the proposed system with previous work (simulation) respectively. It is realized that the proposed IsOWC system using integrated OAM-MDM and improved ZCC code performs better than existing works.

Table 8. Walsh-Hadamard code ($K = 3, W = 2, N = 4$) [23]

User	1550 nm	1550.8nm	1551.6nm	1552.4nm
1st	1	0	1	0
2nd	1	1	0	0
3rd	1	0	0	1

$$chip\ positions = \begin{cases} User\ 1 \rightarrow 1,3 \\ User\ 2 \rightarrow 1,2 \\ User\ 3 \rightarrow 1,4 \end{cases}$$

Table 9. DW code ($K = 4, W = 2, N = 6$) [23]

User	1550 nm	1550.8nm	1551.6nm	1552.4nm	1553.2nm	1554 nm
1st	0	0	0	0	1	1
2nd	0	0	0	1	1	0
3rd	0	1	1	0	0	0
4th	1	1	0	0	0	0

$$chip\ positions = \begin{cases} User\ 1 \rightarrow 5,6 \\ User\ 2 \rightarrow 4,5 \\ User\ 3 \rightarrow 3,4 \\ User\ 4 \rightarrow 1,2 \end{cases}$$

Table 10. Codes' comparison based on codes' properties

Code	Code weight	Code length	No. of users	Cross-correlation
Walsh-Hadamard [23]	2	4	3	2^{M-2} (M= matrix sequence)
DW [23]	2	6	4	1
Improved ZCC [Proposed code]	2	8	4	0

Table 11. Comparative analysis w.r.t. existing works

Ref. (Year)	Implementation	Throughput (Gbps)	Range (km)	Modulation	MDM	Code	Divergence angle	No. of channels	Aperture diameter (cm)	Input power (dBm)	Thermal noise and additional loss	Complexity and cost	BER
[12] (2012)	Simulation	100	9532	QPSK	-	-	2 mrad	1	10	30	-	Moderate	10^{-9}
[10] (2013)	Simulation	2.5	1000	OOK	-	-	2 mrad	1	20	10	-	Low	10^{-9}
[24] (2018)	Simulation	40	2500	Alternate Mark Inversion	-	-	-	64	20	5	-	Moderate	10^{-9}
[13] (2019)	Simulation	10	4500	MDRZ-DQPSK	LG	-	-	64	15	10	-	Moderate	10^{-9}
[15] (2019)	Simulation	40	3750	DPSK	Linearly polarized (LP)	-	-	64	15	10	-	High	10^{-9}
[9] (2021)	Simulation	2	45,000	OOK	-	-	0.75 μrad	16	30	10	-	Low	10^{-6}
[11] (2021)	Simulation	10	1000	BPSK	-	-	-	1	5	-	-	Moderate	10^{-3}
[14] (2024)	Simulation	64	3,600	OOK	-	-	0.75 μrad	16	-	10	-	Moderate	10^{-9}
[25] (2024)	Simulation	3	1,500	OOK	-	-	-	-	25	20	-	Moderate	10^{-9}
[26] (2025)	Simulation	20	6,000	Pulse Amplitude Modulation	-	-	-	-	-	27	-	High	10^{-9}
This work	Simulation	10	36,000	OOK	OAM	Improved ZCC	15 μrad	16	25	20	Yes	Low	10^{-9}

As seen in Table 11, the proposed system offers best performance than existing works in terms of providing maximum inter-satellite link range of 36,000 km at aggregate data rate of 160 Gbps using simple and low cost system design. However, ref. [9] illustrates extended transmission range of 45,000 km than the proposed system, but at the cost of low aggregate data rate of 32 Gbps even after using larger aperture size of 30 cm. Also, the proposed system uses the improved ZCC code to enhance the data security, which is not available in the existing simulations works. By simple modulation scheme (OOK) in the proposed system, it offers faithful data transmission considering the impact of thermal noise, dark current, modal-interference, beam divergence (=15 μrad) and additional loss. At moderate aperture size of 25 cm, the proposed system operating at input power of 20 dBm, it shows better performance than existing works.

In spite of these benefits, the proposed system undergoes different key technical challenges for real-world feasibility. Few major challenges are beam misalignment, pointing errors, atmospheric turbulence (for satellite-ground links), mode crosstalk for higher-order OAM modes, generation as well as detection complexity for large number of end users and link size constraints for transmissions of different OAM modes. To mitigate all challenges and the signal inference between OAM modes, the proposed system requires precise beam tracking, acquisition, and pointing approach, utilization of mode diversity schemes, advanced digital signal processing systems, integration of low-power, compact integrated OAM transceivers and utilization of hybrid multiplexing schemes.

4. Conclusion

A high-speed IsOWC system using integrated MDM-OCDMA scheme at 160 Gbps data rate is designed and investigated. Four different OAM modes are realized for four distinct improved ZCC code sequences offering sixteen active users. It is concluded that the system can sustain maximum spot size of 15 μm with 88.5% eye opening BER patterns and 5.57e-15 watt signal power over a 30,000 km range at Q-factor of 6. Also, the system offers acceptable BER limit upto 0.0022 mrad transmitter and 0.0021 mrad beam divergences. At maximum transmitter and receiver aperture diameters of 50 cm, the system performance can be enhanced multiple times. Besides, transmission range can be extended upto 36,000 km for various OAM beams. Moreover, the system offers high gain of 95.94 dB, low noise figure of -95.94, and high OSNR of 21.45 dB. It is also realized that as compared to DW and haramard codes, the proposed code can provide maximum received power of -7.8 to 14.24 dBm over 0.5-15 dB additional loss with transceiver divergence angle of 15 μrad for 128 numbers of end users over 30000 km. This design offers optimum results compared to exiting works and can be used for future based massive, secure and large distance satellite communications.

References

[1] H. Kaushal, G. Kaddoum, IEEE Commun. Surv. Tut. **19**, 57 (2017).
[2] M. Hadi, M. R. Pakravan, J. Lightwave Technol. **35**, 2853 (2017).
[3] V. Arya, V. Pahwa, R. Kumar, J. Opt. Commun. **0**, 1 (2025).
[4] V. Arya, J. Opt. Commun. **0**, 1 (2025).
[5] V. Arya, S. Gupta, 2025 1st Int. Conf. Radio Freq. Commun. Networks, pp. 1–6 (2025).
[6] V. Arya, K. Roy, Indones. J. Electr. Eng. Comput. Sci. pp. 1–6 (2025).
[7] S. Sachdeva, H. Pahuja, M. Sindhwani, K. Arora, J. Opt. Commun. **45**, s955 (2022).
[8] V. Arya B. M. U. D. Naikoo, 2025 1st Int. Conf. Radio Freq. Commun. Networks pp. 1–6 (2025).
[9] M. M. Tawfik, M. F. A. Sree, M. Abaza, H. H. M. Ghouz, IEEE Photonics J. **13**, 1 (2021).
[10] V. Sharma, N. Kumar, Opt. Commun. **286**, 99 (2013).
[11] A. S. Youssouf, N. F. Hasbullah, N. Saidin, M. H. Habaebi, R. Parthiban, M. R. Bin Mohamed Zin, E. A. A. Elsheikh, F. M. Suliman, PLoS One **16**, 1 (2021).
[12] B. Patnaik, P. K. Sahu, IET Commun. **6**, 2561 (2012).
[13] H. K. Gill, N. S. Grewal, G. K. Walia, Microw. Opt. Technol. Lett. **61**, 1802 (2019).
[14] N. I. Hamadamen, Telecommun. Syst. **86**, 785 (2024).
[15] H. K. Gill, G. K. Walia, N. S. Grewal, Optik **177**, 93 (2019).
[16] Y. Liu, S. Zhao, J. Zhao, X. Li, C. Dong, Y. Zheng, J. Yang, J. Light. Technol. **35**, 3825 (2017).
[17] J. Ji, G. Zhang, W. Li, L. Sun, K. Wang, M. Xu, J. Opt. Commun. Netw. **9**, 813 (2017).
[18] Q. Ding, L. Zheng, H. Liu, J. Li, X. Guo, X. Cheng, Z. Dai, Photonics **9**, 1 (2022).
[19] V. Arya, J. Opt. Commun. **0**, 1 (2025).
[20] M. S. Anuar, S. A. Aljunid, N. M. Saad, S. M. Hamzah, Opt. Commun. **282**, 2659 (2009).
[21] M. Rahmani, A. Cherifi, A. S. Karar, G. N. Sabri, B. S. Bouazza, Photonics **9**, 310 (2022).
[22] H. I. Nur, M. S. Anuar, S. A. Aljunid, M. Zuliyana, 4th Int. Conf. Photonics, ICP 2013 - Conf. Proceeding 237 (2013).
[23] S. A. Aljunid, Z. Zan, S. B. A. Anas, M. K. Abdullah, Malaysian J. Comput. Sci. **17**, 30 (2004).
[24] R. Kaur, H. Kaur, Optik **154**, 755 (2018).
[25] K. Sarker, S. Pradip, M. A. Hossain, Opt. Contin. **3**, 1224 (2024).
[26] A. Gill, G. Gnanagurunathan, N. Khan, J. Opt. Commun. **0**, 1 (2025).

*Corresponding author: meetkumari08@yahoo.in